Large Eddy Simulation of impinging shock wave/turbulent boundary layer interaction at M=2.3

Emmanuel de MARTEL*, Eric GARNIER*, Pierre SAGAUT**

* Office National d'Études et de Recherche Aérospatiales,

BP 72 - 29 Av. de la division Leclerc, 92322 Châtillon cedex, France.

** Laboratoire de Modélisation Mécanique – Université Pierre et Marie Curie

Boite 162 – 4 place Jussieu, 75252 Paris cedex 05, France.

emmanuel.demartel@onera.fr, eric.garnier@onera.fr, sagaut@lmm.jussieu.fr

Abstract. Large eddy simulation (LES) of a bidimensionnal interaction of an oblique shock with a plane plate has been performed for two shock generator angles: 8º and 9.5º. Qualitative agreement is found with experimental results but the length of the interaction is underestimated. Adimensionalisation using the interaction length L as defined by [3] ascertains the statement that L is a characteristic length of the interaction. Frequential analysis leads to the identification of the different regions of the interaction but estimation of low-frequency is not reliable because of the duration of pressure signal available. Delayed detached eddy simulation have also been performed in the entire facility and demonstrate that the role of lateral wall is non negligeable.

Key words: shock wave boundary layer interaction, LES, unsteadiness, three-dimensionality compressible flow.

1. Introduction

Shock wave / turbulent boundary layer interactions (SWTBLI) are involved in manifold internal and external aerothermodynamics problems, such as activated control surface (compression corner), airfoils at transonic flow conditions or incident shock interaction in air intakes for instance. The understanding of physical phenomena associated with unsteady SWTBLI motivates the aerospace research community since they can lead to aircraft performance degradation, structural fatigue or air intake efficiency reduction. In this study, we will concentrate on the reflection of an incident shock wave impinging on a boundary layer developing on a plate plane.

Main characteristics of SWTBLI can be found in Delery and Marvin [1] and Smits and Dussauge [2]. Experiments show that if the shock intensity is strong enough to make the boundary layer separate, the foot of the reflected shock oscillate at very low frequency compared with the characteristic temporal scales of the incoming boundary layer. The possible coupling between low frequency shock motion, unsteadiness of the separated bubble and vortex shedding in the separated zone has to be clarified. Upon this point, a recent experimental work

involving shock reflection, realised by Dupont *et al*. [3] at the *Institut Universitaire des Systèmes Thermiques Industriels* (IUSTI), highlighted a high level of coherence at low frequencies between the vicinity of the reflected shock and near the reattachment region. Pirozzoli *et al*. [4] suggest also a mechanism involving acoustic waves to explain the oscillatory motion of the separation bubble and the subsequent flapping motion of the reflected shock. The question of the origin of the instability is therefore still open.

In an extended review, Dolling [5] pointed out that Large Eddy Simulation (LES), associated with experiments, should bring more understanding of the unsteady phenomena involved in SWTBLI. In a first attempt to treat the case of the interaction of an oblique shock impinging on the boundary layer developing on a flat plate (the IUSTI case with a shock deflection of 8 degrees), Garnier *et al.* [6] have found that LES can be considered as a predictive tool to simulate such a physically complex flow. A satisfactory agreement with experimental data was found for mean and fluctuating longitudinal velocity and the separated zone was correctly described by the simulation. Nevertheless, the duration of the computation was insufficient to study the low-frequencies in the interaction.

In this study, we investigate the effect of the shock angle by computing two cases of shock deflection well documented by IUSTI. More signal than in [6] is acquired and the influence of the wind tunnel side walls is investigated.

2.   Numerical Method

The FLU3M code developed by ONERA has been used to solve the Navier-Stokes equation. A second-order accurate Roe scheme modified with the Ducros *et al*. [7] sensor is used for spatial discretization whereas time discretization is based on second-order Gear's formulation as presented by Pechier *et al*. [8].

In Large-Eddy Simulation (LES), the large-scales field is computed directly from the solution of the filtered Navier-Stokes equations and the unresolved scales are modeled by means of a subgrid scale (SGS) model. More details about the selective mixed scale model used in present computations can be found in [9].

Delayed Detached Eddy Simulation (D-DES) has also been used in computations with lateral wall to limit the cost of the computation. This hybrid RANS (Reynolds-Averaged Navier Stokes modeling)/LES approach is based on the DES originally proposed by Spalart *et al*. [10], in which a delay function [11] is used to force attached boundary layer to be treated with RANS modeling.

3.   Description of the configuration

3.1   EXPERIMENTAL SETUP

The experiment was carried out in the low turbulence supersonic wind tunnel at the IUSTI. The test section is 17 cm wide and 12 cm high. The free-stream Mach number is 2.3. Upstream the interaction the incoming boundary layer has a thickness δ_0 of 11 mm, an incompressible momentum thickness θ of 1.28 mm and a Reynolds number based on it Re_θ of 6900. The skin friction coefficient C_f is equal to 0.002 and the total temperature T_t is equal to 300 K.

The shock is generated by a sharp-edged plate fixed to the upper wall of the wind tunnel. It interacts with the turbulent boundary layer which develops on the lower plate. Several angle of shock generator have been tested. In this study, we focus shock generator angles of 8 and 9.5 degrees. A particularity of this experimental setup is that theoretical shock impingement position on the plane plate is located at constant position whatever the shock generator angle.

3.2 SIMULATIONS OVERVIEW

Two LES with angles of generator equal to 8 and 9.5 degrees have been carried out, using periodic lateral conditions and the same numerical parameters. The computational domain (Figure 1) is 25 δ_0 long, 1.8 δ_0 wide and 8.7 δ_0 high. 10 δ_0 are used to stretch the mesh before the outlet. A 3D/2D split occurs 2.5 δ_0 from the lower plate. A 10 δ_0 long precursor domain is used to generate inflow conditions. An outflow domain to the precursor avoid that possible perturbation due to the interaction enter into the precursor. The total grid contains about 4.5 million points. Cells resolution at the lower plate is 50x18x1 wall unit in the streamwise, spanwise and wall-normal direction. The time step is $0.4 \cdot 10^{-7}$ s.

In order to take into account the effect of lateral wall (see section 5.2), the whole experimental set up (Figure 2, top) was first computed with a RANS approach. The shock generator was modelized by a slip condition at the boundary between the red and the green domain. Then, DDES was performed only downstream of the domain corresponding to the nozzle (Figure 2, bottom, in light blue) to limit the computational cost (since the flow is supersonic). In order to prevent DDES from spurious behavior in wall corner, separated grid have been set along the side wall, up to three δ_0 from the side wall. These grids are explicitly computed with RANS approach. Cells resolution at the lower plate is 50x50x1 wall unit in the streamwise, spanwise and wall-normal direction. The computed grid contains 18 million points, dispatched on two processors. The timestep is $0.4 \cdot 10^{-7}$ s.

4   Inflow conditions

As mentioned above, LES computations need a precursor domain to generate inflow conditions. The recirculating and rescaling method of Lund *et al*. [12] adapted to compressible flow [13] has been used here. The general idea is to decompose each flowfield component into a mean and a fluctuating part.

Fluctuations at a downstream station are rescaled and reintroduced at the inflow boundary. The appropriate scaling law is there applied for inner and outer region of the boundary layer.

Streamwise velocity profiles extracted from the simulation and hot-wire (HW) data before the interaction at x = 260 mm are plotted in Figure 3. Usual Van Driest transform of mean velocity profiles is used to compare computations and wind-tunnel experiments:

It is to be noticed that the experimental skin friction is not measured but evaluated assuming the profile follows the classical law ln(z+)/0.41+5.25. This explains the perfect agreement of the experimental profile with this law. Computation exhibits an overestimation of U_{vd} in the logarithmic zone. As skin friction coefficient of the simulation is very close to the experimental one (both coefficient are equal to 0.002), this is due to a fuller profile than the experimental one in the log law.

Streamwise velocity fluctuations are plotted in figure 4. They have been adimensionalized by the friction velocity and multiplied by density. This allows to take into account the effects of kinetic heating and to compare compressible and incompressible data. The results are better than in [6] in the first half of the boundary layer but an overestimation of fluctuations is observed in the second half of the boundary layer. The maximum of fluctuations reaches 3.3 near the wall whereas the value of 3.2 was obtained in [6]. This is consistent with the fact that the friction coefficient was underestimated in this previous work.

5   Results

5.1   LES WITH LATERAL PERIODIC CONDITIONS

5.1.1   General Results

The two Large Eddy Simulations performed with shock generator angle of 8° and 9.5° exhibit a separation with an underestimation of the interaction length L. The latter is defined following Dupont *et al.* [3] as the distance between the mean position X_0 of the reflected shock and the extrapolation to the wall of the incident shock wave X_1. This length is roughly the length between the reflected shock and the reattachment point. In the 8° case, the computational interaction length is 22 millimeters instead of 46 millimeters in the experiment and in the 9.5 degree case, this length is 40 millimeters instead of 71 millimeters.

As mentioned in section 5.1.4, the lack of spanwise extension in these simulations does not explain this behaviour since the same results are obtained with a span of 100 millimeters. However, these results have to be taken with care because the simulations do not take into account side wall effects which are non negligible, as it will be seen in section 5.2.

4

Nevertheless, results in the 8° case can be compared with results of Garnier *et al.* [6] in similar condition regarding span as they also used periodic condition with a computational domain width of 15 millimeters. They found a good agreement for the length of separation but with simulations that underestimates the friction coefficient by 10 %. This, together with the discrepancies registered in the velocity profile (too full), may explain the differences observed on the length of separation.

5.1.2   Statistical analysis

Despite discrepancies between the computational and experimental interaction length, it appears that using the adimensionalization $X^*=(x-X_0)/L$ as in [3] allows us to compare experimental and computational data. Figure 5 and 6 show the longitudinal evolution of mean pressure P and standard deviation pressure P_{rms} = $(<P'^2>)^{1/2}$. The dimensionless values are defined by: $P^* = (P-p_1) / (p_2-p_1)$ and P'^* = $P_{rms} / (p_2-p_1)$, where p_1 and p_2 are respectively the pressure upstream and downstream of the incident shock, both deduced from the inviscid theory. The raise of the mean pressure in the vicinity of the reflected shock foot is sharper than in experimental data for both cases. This is due to a smallest amplitude of shock motion in the computations. As a consequence, time averaged pressures undergo a sweep effect over a smaller length in comparison with experiments, hence the sharper increase. This discrepancy is emphasized in the 9.5° case because experimental amplitude of shock motion is higher than in the 8° case. The r.m.s. pressure presents a bump at the mean position of the reflected shock ($X^*=0$). In order to compare computational and experimental data, r.m.s. pressure obtained from LES have been filtered to 20 kHz which correspond to the cut off frequency of the Kulite transducer. Levels of fluctuations before the interaction are significantly overestimated by the computation. The maximum levels reached in bump are underestimated, especially in the 9.5° case. This can be due to the overestimation of the turbulence level which strengthens the boundary layer before the interaction and may contributes to reducing the separation and the unsteadiness in the reflected shock. In the relaxation zone, the level of pressure fluctuation is satisfactorily estimated.

Despite a significant discrepancy between experiments and LES for both angles of shock generator in term of interaction length, adimensionalisation using L in the dimensionless coordinate X^* was proved to be efficient. This ascertains the statement of Dupont *et al.* [3] that L is a characteristic length for a wide range of interaction, at least in the initial part of the interaction.

LES comparisons between the two shock generator angles are therefore possible, using this adimensionalisation. Figure 7 show isovalues of mean longitudinal velocity for 8° (top) and 9.5° (bottom) cases, using X^*. Wall-normal coordinate is divided by δ_0. Separation line (isovalue of longitudinal velocity U=0 m·s^{-1}) has also been plotted. The 9.5° case exhibits a longer and higher separated flow than the 8° case, which is in qualitative agreement with experiments. The interaction

length is also more important than in the 8º case. In the same manner, Figure 8 presents fluctuations levels of wall-normal velocity. The maximum level reached in the interaction is 118 m·s^{-1}, respectively 122 m·s^{-1}, in the 8º, respectively 9.5º case. The raise of turbulent fluctuations presents a larger extension in the 9.5º case than in the 8º case. This is consistent with the fact that present simulations present a qualitative agreement with experiments.

5.1.3   Frequential analysis

As mentioned before, the length of interaction L is underestimated in LES with the two angles of shock generator (8º and 9.5º). However, a qualitative agreement with experiment seems to be reached. In order to go into further details, the power spectral densities of wall pressure signals estimated for positions ranging from the upstream flow to the relaxation have been estimated. The results are presented on figure 9 for the 8 degrees case and in figure 10 for the 9.5 degrees case.

The chosen representation for spectra is f·E(f) where E is the PSD normalized to unity (E has been divided by the total energy for each position). In both cases the wall pressure signal have been recorded with a sample frequency of 192 kHz during 20.08 ms. Experiment shows that the low frequency of shock motion is expected to be of the order of 200 Hz and 420 Hz, in 9.5 degrees case and in the 8 degrees respectively. The duration of the simulation corresponds only to 4 or 8.4 periods depending of the case.

In both simulations, high frequencies can be identified in the incoming boundary layer. The reflected shock position around $X^* = 0$ is then characterized by low frequencies and is followed by the interaction zone until $X^* = 1$ associated with intermediate scales in the frequency range (1kHz-10kHz). Qualitatively this reproduces what can be found in the experiments. Nevertheless, the same frequency of about 200 Hz at the foot of the reflected shock has been identified in the two cases 8 and 9.5 degrees. The fact that the frequency remains unchanged when the shock angle rises is still not explained but one has to notice that the accuracy of these pressure power spectral densities is limited by the available length of wall pressure signals.

5.1.4   Role of span extension

In order to investigate the role of spanwise extension, a similar simulation has been performed with a spanwise extension of 10 centimeters, for the 9.5 degrees case. This extension was chosen to let enough space for contrarotative vortices to develop, as observed experimentally. The results of this simulation did not show significant differences with present small span simulation. In particular, it did not exhibit any contrarotative vortices and the length of interaction was nearly unchanged.

5.2   COMPUTATIONS WITH LATERAL WALL

In order to investigate side wall effects on the interaction, computation of the whole wind-tunnel has been performed using a RANS approach in a first step. The angle of shock generator was set to 9.5º. Figure 11 presents the tridimensionality of the flow field in the interaction, hence the shock generator (in black), the incident shock (iso pressure 5100 Pa, in light blue), the recirculation (iso streamwise velocity equal to 0 m·s^{-1}, in brown) and the wall pressure on the lower plate. The topology of the interaction is clearly three-dimensional. In particular, the shape of the incident shock wave is strongly distorted in the lower side corners, where large recirculations appear too. According to this simulation, it seems that getting the physic of the interaction implies to take into account side wall effect.

DDES of this configuration is now in progress to investigate unsteadiness of the interaction. No turbulent inflow condition has been used there. First results yield a length of interaction of 89 millimeters along the median line where experimental data are available, instead of 71 millimeters. The reason of this overestimation remains to be explained. A spurious behaviour of SA model in side wall regions which have been treated with RANS may explained these discrepancies. Unfortunately experimental data are not available near the side walls. Furthermore, on the contrary to previous 2D LES, contrarotative vortices appear in the separated bubble. This underlines the need of taking into account lateral walls in the simulation of the interaction. Figure 12 presents an instantaneous field of current DDES. The incident shock below the shock generator (in black) is represented by lines iso Mach number equal 2 (in blue). This shows the warped incident shock near lateral wall. Isosurface of the Q criterion (pink) is plotted in a half side of the domain whereas recirculation (in brown) is plotted in the second half. Wall pressure is also represented, underlining the three-dimensionality of the interaction.

6   Conclusion

Bi-dimensional interaction of an oblique shock impinging on a plane plate has been studied with shock generator angles of 8º and 9.5º using LES. The Lund *et al.* [12] methodology has been used to generate inflow conditions. The use of this technique permits to recover the correct skin friction coefficient and a satisfactory evolution of the streamwise velocity fluctuations in the first half of the boundary layer. However, an overestimation of the fluctuations is observed in its second half. Despite discrepancies on the interaction length, LES and experimental data are in qualitative agreement. The longitudinal evolution of mean and standard deviation pressure using the dimensionless coordinate X* is correctly reproduced by LES. This ascertains the statement that the interaction

length is the characteristic scale of the interaction. Frequential analysis has allowed us to identify regions of the interaction associated with different time scale as in [3]. However, the available duration of wall pressure signal has not permitted to provide reliable results on low-frequencies.

Simulation of the entire facility has pointed out the role of lateral walls in the interaction. Such a simulation leads to a better quantitative agreement with experimental data. However, cost limitation imposes the use of a hybrid RANS/LES approach for which a particular treatment of the corners has been employed. The accuracy of this computation strategy is still to be demonstrated.

Acknowledgements
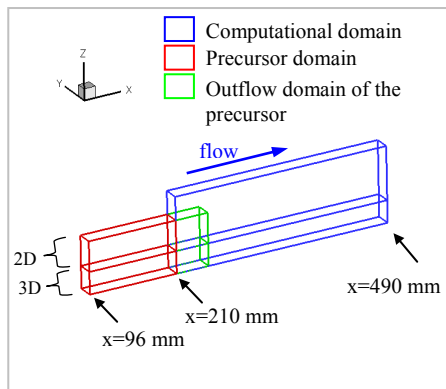
Figures

Figure 1: grid organization of LES computations
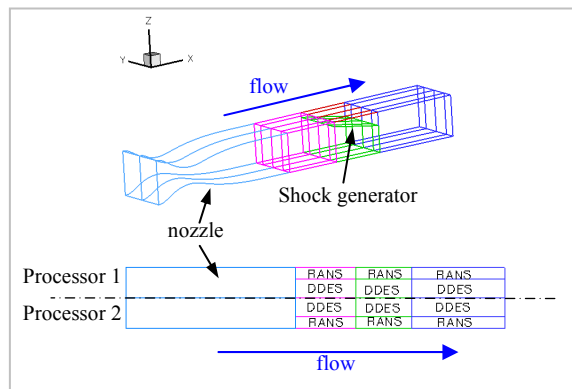
Figure 2: overview of DDES grid. Top: general configuration. Bottom: top view of the computational domain.
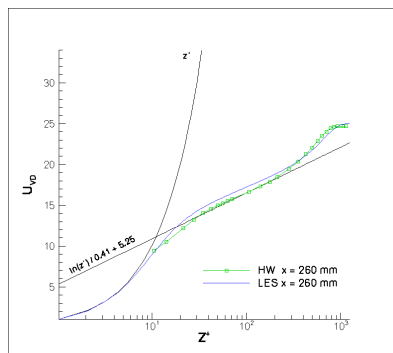
Figure 3: Van Driest transformed inflow mean velocity
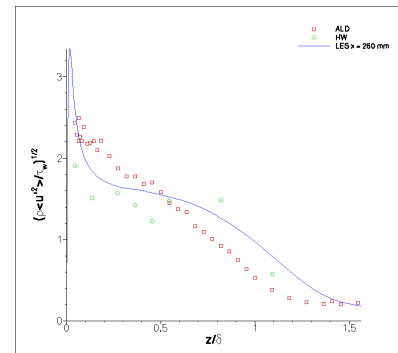
Figure 4: Inflow streamwise velocity fluctuation

8
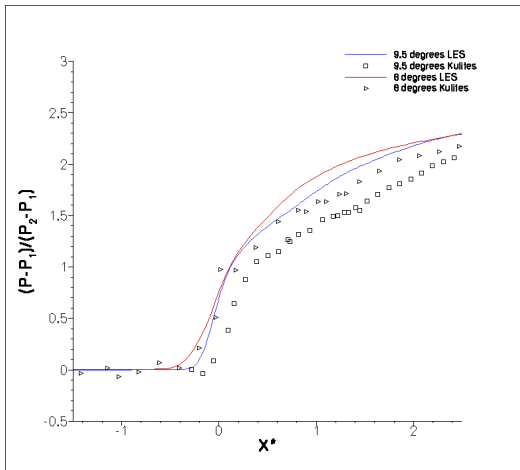
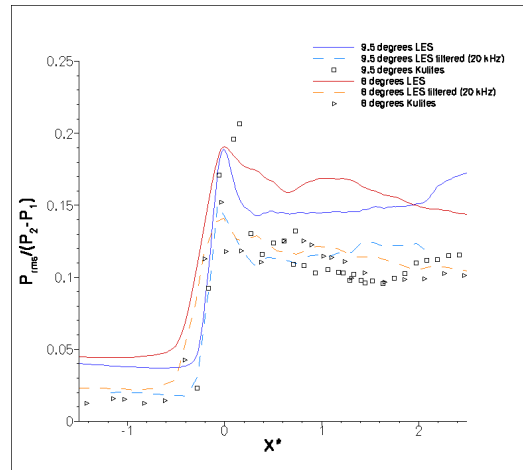Figure 5: Longitudinal evolution of mean pressure

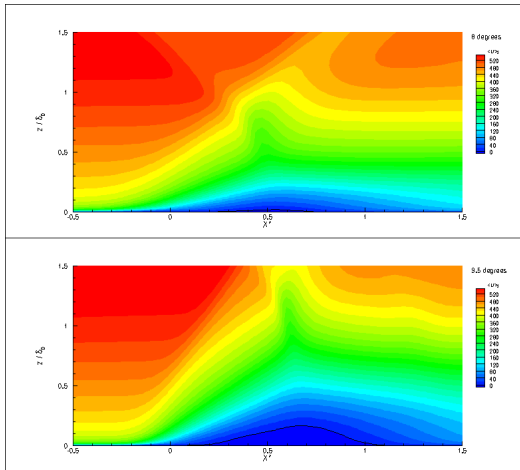Figure 6: Longitudinal evolution of mean pressure

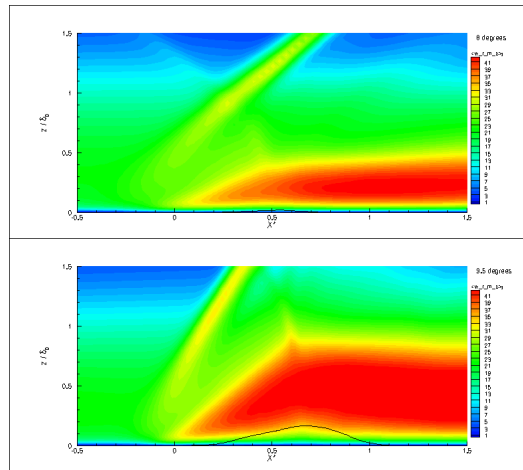Figure 7: mean longitudinal velocity and separation line (in black).

Figure 8: mean wall-normal velocity fluctuations and separation line (in black).
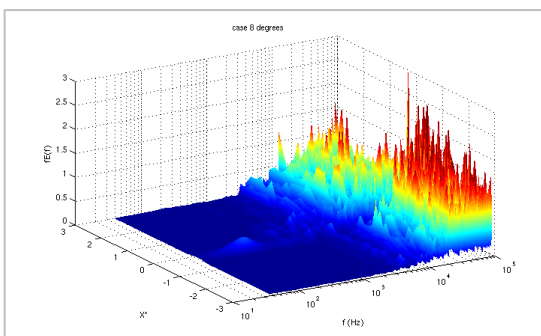

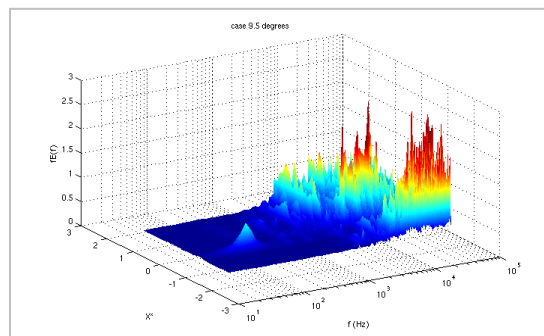Figure 9: Pressure power spectral density along the interaction (angle: 8º)

Figure 10: Pressure power spectral density along the interaction (angle: 9.5º)
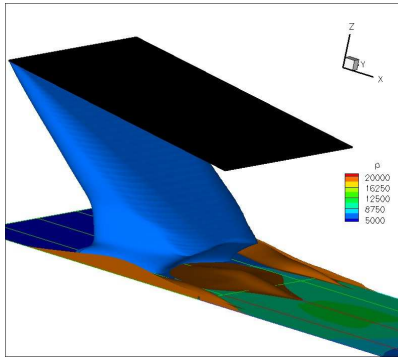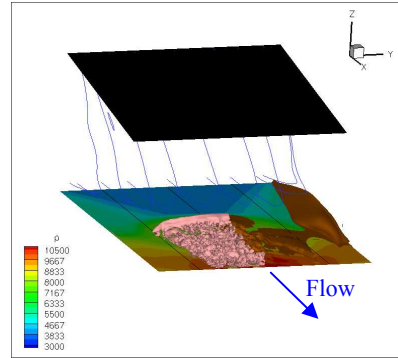
Figure 11: RANS simulation with side wall.

Figure 12: DDES simulation with side wall.

References.

1. Delery J. and Marvin G. J., Shock-Wave Boundary Layer Interactions. *AGARDograph 280*, (1986), 51-55.
2. Smits A. J. and Dussauge J. P., Turbulent Shear Layer in Supersonic Flow. *AIP Press*, Woodbury, NY (1996), 285-319.
3. Dupont P., Haddad C. and Debieve J.F., Space and time organisation in a shock-induced separated boundary layer. *J. Fluid. Mech. 559* (2006), 255-277.
4. Pirozzoli S. and Grasso F., Direct Numerical Simulation of Impinging Shock Wave / Turbulent Boundary Layer Interaction at M=2.25. *Phys. of Fluids 18* (2006), 065113.
5. Dolling, D.S., Fifty Years of Shock-Wave/Boundary Layer Interaction Research: What Next? *AAIA Journal 39*, No.8 (2001), 1517-1531
6. Garnier E., Sagaut P., Deville M., Large Eddy Simulation of Shock/Boundary-Layer Interaction. *AIAA Journal 40*, No. 10 (2002), 1935-1944.
7. Ducros F., Ferrand V., Nicoud F., Weber C., Darracq D., Gacherieu C. and Poinsot T., Large-Eddy Simulation of Shock/Turbulence Interaction. *J. Comput. Phys. 152* (1999), 517-549.
8. Pechier M., Guillen P. and Cayzac R., Magnus Effect Over Finned Projectiles. *Journal of Spacecraft and Rockets 38*, No. 4 (2001), 542-549.
9. Lenormand E., Sagaut P., TA Phuoc L. and Comte P., Subgrid-Scale Models for Large-Eddy Simulation of Compressible Wall Bounded Flows. *AIAA J. 38* (2000), 1340-1350.
10. Spalart P. R., Jou W. H., Strelets M. and Allmaras S.R., Comments on the Feasibility of LES for Wings and on a Hybrid RANS/LES Approach. *Proceedings of the 1st AFSOR International Conference on DNS/LES*, Greyden Press, Colombus, OH (1997), 137-147.
11. Spalart P. R., Deck S., Shur M. L., Squires K. D., Strelets M. Kh and Travin A., A New Version of Detached-Eddy Simulation, Resistant to Ambiguous Grid Densities. *Theoritical and Computational Fluid Dynamics 20* (2006), 181-195.
12. Lund T. S., Wu X. And Squires K. D., Generation of Turbulent Inflow Data for Spatially-Developping boundary Layer Simulations. *Journal of Computational Physics 140*, No. 2 (1998), 233-258.
13. Urbin G. and Knight D., Compressible Large Eddy Simulation Using Unstructured Grid : Unstructured Boundary Layer. *Second AFSOR Conference on DNS/LES*, Kluwer Academic, Norwell, MA, (1999), 443-458.